Physics and Chemistry of the Earth 144 (2026) 104527

Contents lists available at ScienceDirect

Physics and Chemistry of the Earth

journal homepage: www.elsevier.com/locate/pce

Seismotectonics and fault kinematics of the Zagros fold-thrust belt in northeastern Iraq: Constraints from moment tensor inversions and active fault mapping

Emad H. Al-Khersan [a], Suad Mohammed Ali [b], Raad Z. Homod [c,*], Haider H. Dahm [d,e], Mahmood A. Al-Shareeda [f,i], Krishna K. Yadav [g,h]

[a] Shatt Al-Arab University College, Basra, Iraq
[b] Department of Geology, College of Sciences, University of Basrah, Iraq
[c] Department of Oil and Gas Engineering, Basrah University for Oil and Gas, Basra, 1004, Iraq
[d] Department of Civil Engineering, College of Engineering, University of Manara, Iraq
[e] Department of Petroleum Engineering, College of Engineering, University of Misan, Iraq
[f] Basra Technical Institute, Southern Technical University, Basra, 61001, Iraq
[g] Department of VLSI Microelectronics, Saveetha School of Engineering, Saveetha Institute of Medical and Technical Sciences, SIMATS, Saveetha University, Chennai, Tamil Nadu, 602105, India
[h] Environmental and Atmospheric Sciences Research Group, Scientific Research Center, Al-Ayen University, Nasiriyah, Thi-Qar, Iraq
[i] College of Engineering, Al-Ayen University, Thi-Qar, 64001, Iraq

ARTICLE INFO

Keywords:
ZFTB
Arabian–Eurasian convergence
Seismotectonic
Active fault systems
Moment tensor inversions
Hydrocarbon exploration

ABSTRACT

This study examines the seismotectonic framework of the Zagros Fold-Thrust Belt in northeastern Iraq and southeastern Turkey, focusing on Arabian-Eurasian plate convergence and regional seismicity. Using historical earthquake records (1900–2012, $M \geq 3.0$), agency data, and moment tensor inversions from 32 stations, we identify five active fault systems: Khanaqin, Diyala, Şırnak, Hakkari, and a transboundary system into western Iran. Results show reverse and strike-slip faulting at depths of 14–28 km, driven by NW-SE compressional stresses. Moment tensor solutions, derived with region-specific Green's functions and a 1D velocity model, constrain fault kinematics and the stress field. Due to sparse seismic coverage in the Iraqi Zagros, this study relies on only six well-constrained events (Mw 3.5–4.9). Thus, findings are a preliminary, data-limited characterization of local fault kinematics. The scope is descriptive seismotectonic characterization and preliminary structural interpretation, rather than quantitative hazard assessment or full petroleum system analysis. Our integrated approach combines seismic analysis, focal mechanisms, satellite imagery, and historical data to provide a preliminary, data-constrained characterization of active fault kinematics in northeastern Iraq. While based on a limited dataset of six well-constrained events due to sparse regional network coverage, this study provides the first reliable focal mechanisms for the Iraqi Zagros and demonstrates a replicable methodology for future investigations. This work provides one of the first attempts to integrate moment tensor solutions with historical seismicity and structural data across this transboundary region, linking fault kinematics to seismotectonic characterization. Based on structural geometry, reactivated listric faults may influence hydrocarbon trap integrity, but this interpretation is speculative and requires validation by subsurface data.

1. Introduction

The Sulaymaniyah region in northeastern Iraq, situated within the seismically active (ZFTB), occupies a critical position along the continental collision boundary between the Arabian Plate (AP) and Eurasian Plate. This convergence zone represents one of Earth's most tectonically active regions, as demonstrated by numerous studies (Buday et al., 1987), (Numan, 1997), and (Rakib et al., 2026). This belt is one of Earth's most active continental collision zones—a natural laboratory where ongoing plate convergence drives both devastating earthquakes

* Corresponding author.
E-mail addresses: emad.alkhersan@sa-uc.edu.iq (E.H. Al-Khersan), suad.abdsuad@gmail.com (S.M. Ali), raadahmood@yahoo.com (R.Z. Homod), haiderdahm@uomanara.edu.iq (H.H. Dahm), mahmood.alshareedah@stu.edu.iq (M.A. Al-Shareeda), envirokrishna@gmail.com (K.K. Yadav).

https://doi.org/10.1016/j.pce.2026.104527
Received 9 February 2026; Received in revised form 25 April 2026; Accepted 26 May 2026
Available online 28 May 2026

and the formation of world-class hydrocarbon reservoirs. Emphasizing this dual societal and economic relevance from the outset would better engage a diverse audience and set the stage for the study's integrated seismotectonic and petroleum-systems approach.

The present study investigates the seismotectonic characteristics of this area through a comprehensive analysis of seismic history, spatial distribution of earthquake epicenters, and focal mechanism solutions. Particular attention is given to the earthquake that occurred on November 12, 2017. As one of the Earth's most active continental collision zones, the ZFTB serves as a natural laboratory for studying crustal deformation, seismogenic processes, and the interplay between tectonics and hydrocarbon systems; therefore, improved characterization of its fault kinematics and stress regimes has broad implications for seismic hazard assessment and energy exploration.

The earthquake has a magnitude of 7.3 along the Iraq-Iran border, and its focal mechanism and associated crustal structure are examined in detail. Our methodological approach integrates multiple advanced techniques: joint inversion of teleseismic P-wave receiver functions and surface wave group velocity dispersion for crustal structure analysis, along with moment tensor inversion for fault mechanism determination. Additionally, we calculate region-specific Green's functions to enhance the accuracy of moment tensor solutions, enabling precise characterization of fault movement patterns. The study area encompasses the Sulaymaniyah Governorate located between longitudes 42° 25′ 00″ E – 47° 00′ 00″ E and latitudes 34° 55′ 00″ N - 38°00′00″ N, including Sulaymaniyah Station with coordinates of 45.36°N and 35.57°E inside the High Folded Zone (Fig. 1). This investigation provides crucial insights into the active deformation processes in this complex collision zone, with important implications for seismic hazard assessment in northeastern Iraq and surrounding regions.

Given the sparse seismic network coverage in the Iraqi Zagros, this study is necessarily based on a limited set of well-constrained earthquake events (only six moment tensor solutions, Mw 3.5–4.9). Therefore, the findings should be viewed as a preliminary and data-limited characterization of local fault kinematics. Accordingly, the actual scope of this work is a descriptive seismotectonic characterization and a preliminary structural interpretation of active faults, rather than a quantitative seismic hazard assessment or a full petroleum system analysis.

Unlike prior regional studies that focused on crustal structure, individual earthquake analyses, or stress fields, often concentrated in the Iranian sector, this work integrates a new catalog of six well-constrained moment tensor solutions (Mw $\geq$ 3.5) with historical seismicity, remote sensing, and structural analysis. It represents one of the first attempts to develop a unified, transboundary model of active deformation in the Iraqi segment of the ZFTB. The specific gap addressed is the absence of a comprehensive framework that simultaneously characterizes fault kinematics and the contemporary stress regime to directly link active deformation in this underexplored yet tectonically vital border region.

Unlike previous regional studies that focused on individual large earthquakes (e.g., the 2017 Mw 7.3 event), crustal structure, or stress fields predominantly in the Iranian sector (Abdulnaby et al., 2013; Nissen et al., 2023; Gürbüz and Sipahioglu, 2024), the Iraqi segment of the ZFTB remains characterized by sparse, well-constrained focal mechanisms and lacks an integrated transboundary fault model. This study fills that gap by: (1) providing a catalog of six robust moment tensor solutions for moderate-magnitude events (Mw 3.5–4.9) in the under-monitored Iraq-Turkey-Iran border region (2) integrating these with historical seismicity, remote sensing, and structural analysis to produce a unified map of five active fault systems across this transboundary zone, one of the first such attempts for this region; and (3) explicitly linking the reactivation of listric faults (documented via seismological and structural data) to speculative hydrocarbon trap integrity, an integrated approach not previously attempted for this segment.

This study pursues two interconnected objectives: characterizing the seismotectonic framework by identifying active fault systems, determining their kinematics (reverse vs. strike-slip), and constraining the contemporary crustal stress regime; and evaluating how active deformation processes, particularly the reactivation of inherited listric faults control structural trap development, reservoir compartmentalization, and fracture networks, thereby directly impacting hydrocarbon potential. To achieve these aims, a new catalog of six well-constrained

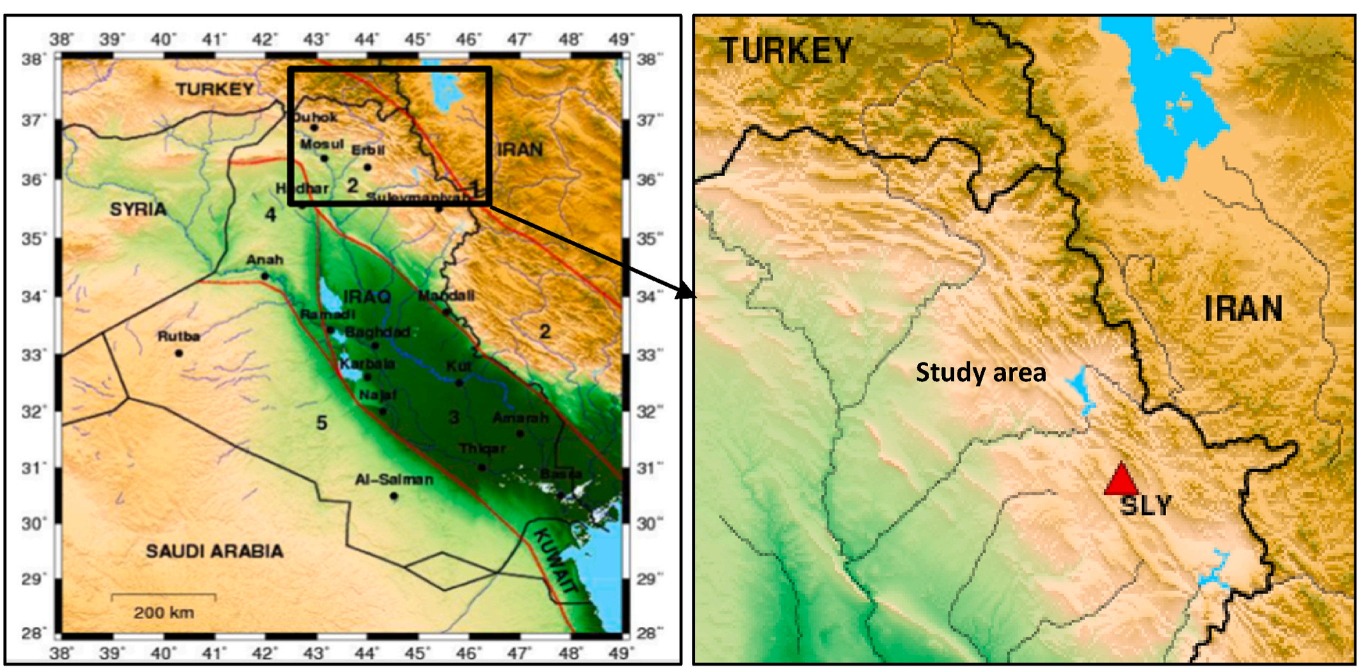

Fig. 1. Location map of the study area. The Sulaymaniyah seismic station (SLY, red triangle) sits within the High Folded Zone of the ZFTB, ideally positioned to record seismicity from the active collision between the Arabian and Eurasian plates. This map establishes the geographic and tectonic context for integrating seismic data across the Iraq-Iran-Turkey border region. (For interpretation of the references to colour in this figure legend, the reader is referred to the Web version of this article.)

moment tensor solutions for moderate-magnitude events (Mw $\geq$ 3.5) is integrated with extensive historical records and remote sensing data, enabling precise determination of fault kinematics and characterization of the contemporary stress regime from focal mechanisms, which yields critical insights into fault permeability, trap integrity, and the orientation of natural fracture networks that enhance reservoir quality. By integrating seismological constraints with structural analysis, this study establishes how active deformation simultaneously governs petroleum system dynamics in this underexplored collision zone, offering a unified model of crustal deformation that links these two domains as illustrated in Fig. 2. The primary contributions of this study are the provision of new moment tensor solutions for the region, the integration of these with historical data to refine fault kinematics, and the development of a multidisciplinary framework that connects active deformation to petroleum system dynamics.

Despite the significance of the ZFTB as an active continental collision zone, the geometry, kinematics, and seismic potential of many fault systems in its Iraqi segment remain poorly constrained due to limited dense seismic monitoring and detailed tectonic studies along the Iraq-Iran border. Key unresolved issues include the partitioning of deformation between reverse and strike-slip faulting at depth, the influence of reactivated basement structures (e.g., listric faults) on both seismogenesis and hydrocarbon trap formation, and the transboundary connectivity of active faults. Moreover, the link between contemporary crustal stresses derived from seismic data and the belt's long-term structural evolution is not fully understood. This study addresses these gaps by integrating new seismological data and advanced analytical methods to deliver a unified model of active deformation, with critical implications for petroleum exploration in this underexplored yet tectonically vital region. Accordingly, this study aims to integrate new seismological data and structural analysis to characterize active fault kinematics and the contemporary stress regime in the ZFTB, thereby establishing how active deformation simultaneously controls petroleum system dynamics in this underexplored collision zone.

2. Related work

This research focuses on investigating the seismicity patterns and active fault systems in the Sulaymaniyah region of northeastern Iraq and surrounding areas within the ZFTB. Over the past century, numerous geophysical and geological studies have sought to understand continental deformation mechanisms in the Zagros orogenic belt, with most research concentrated on the Iranian sector due to limited data from the Iraq-Iran border region, (Table .1).

3. Tectonic settings

Numerous tectonic studies, including (Johnson, 1998), indicate that approximately 95% of Iraq's territory lies within the northeastern Arabian Platform, with only a minor portion extending into the Eurasian (Iranian) Plate. The AP, encompassing Syria, Jordan, Iraq, and western Iran, began separating from Africa during the Miocene through continental rifting along the margin of northeast Africa, leading to the formation of the Red Sea and Gulf of Aden (Sissakian et al., 2014). This north/northeast-moving plate (Al-Sinawi, 2002) subsequently collided with the Eurasian Plate, forming major mountain ranges including the Zagros, Alborz, Pyrenees, and Himalayas (Sharland et al., 2001). The AP's geological evolution includes the Nabitah Orogeny (680-640 Ma), Permian crustal extension that separated Iranian terranes and opened the Neo-Tethys, and a passive margin phase from late Permian to Cretaceous (Fouad, 2008). Formerly part of the African Plate throughout the Phanerozoic until the Oligocene (Rakib et al., 2026), Iraq now occupies the AP's northeastern edge where Zagros-related deformation propagates southwestward. Iraqi tectonic zonation schemes (following (Fouad, 2012a), (Fouad, , 2012b), and (Onur et al., 2017) divide the country into an inner platform (stable zone) and an outer platform comprising the Mesopotamia Foredeep and ZFTB, which is our study area. The ZFTB, resulting from Late Cretaceous Arabian-Eurasian convergence, contains thick folded/faulted Paleozoic-Cenozoic sequences subdivided northeast-to-southwest into: Thrust Zone, Imbricate Zone, High Folded Zone (folded belt), and Low Folded Zone (foothills) (Fig. 3).

4. Data acquiring and methodology

The data used in this study were obtained from two primary sources: (1) Earthquake metadata from the International Seismological Centre (ISC), which were used to analyze the seismic history of active faults and (2) Waveform seismic data from MP stations in Iraq and the Kandilli Observatory and Earthquake Research Institute (KOERI) in Turkey, which were utilized for focal mechanism solutions.

Several specialized programs were employed for earthquake data processing. There are.

- Computer Programs in Seismology (CPS) version 3.30, installed on a LINUX platform, contains over 140 programs, many of which were scripted by Herrmann for tasks such as seismic data preparation and inversion. The CPS was primarily used for calculating focal mechanism solutions.

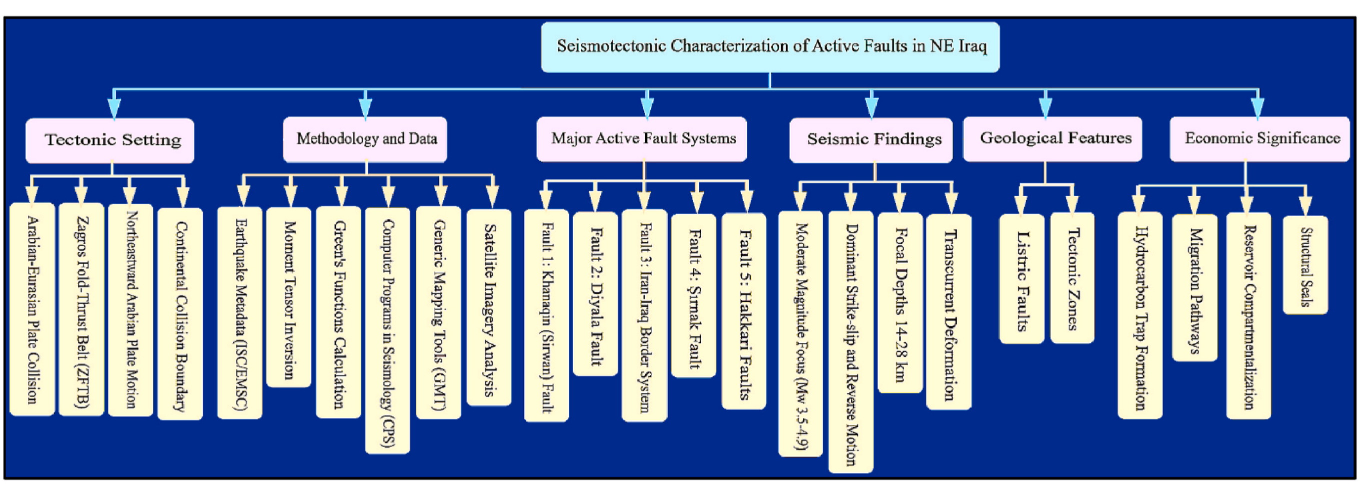

Fig. 2. Flowchart of the integrated methodology. This workflow shows how the study combines moment tensor inversions, historical seismicity, and remote sensing to achieve two interconnected goals: characterizing active fault kinematics and linking the reactivation of listric faults to hydrocarbon trap formation. The chart illustrates the unified framework connecting active deformation to both seismic risk and petroleum system dynamics.

Table 1
Summarizes previous and recent research relevant to the present study.

Authors	Abstracts
Al-Khersan et al., 2010	Paleomagnetic studies provided critical insights into the tectonic evolution of northern Iraq, demonstrating that the Neotethys ocean persisted during the Maastrichtian before closing between the Maastrichtian and Lower Tertiary periods. This closure, driven by the northeastward rotation of the Afro-AP, generated significant latitudinal movement (approximately 20°) and triggered widespread faulting and seismic activity
Abdulnaby et al. (2013)	Established northern Iraq as part of the active Arabian-Eurasian plate boundary, characterized by dominant strike-slip mechanisms with reverse components at focal depths of 15-25 km, and identified three principal stress directions (N–S, NE-SW, and E-W) consistent with regional tectonics
Abdulnaby et al. (2020)	Expanded this understanding through analysis of twelve seismic stations, highlighting the persistent seismic hazard exemplified by events like the 2017, magnitude 7.3 earthquake, which underscores the ongoing tectonic activity in this fold and thrust belt region.
Nissen et al. (2023)	The November 2017 Mw 7.3 earthquake, one of the largest instrumental events in the Zagros, involved a complex rupture process modeled using InSAR and teleseismic waveforms. The preferred model reveals a high-angle reverse fault that ruptured a previously unidentified blind structure in the lower sedimentary cover, underscoring the challenge of mapping seismogenic faults in the Zagros and the significant seismic hazard posed by blind thrusts.
Naderi and Karimzadeh (2024)	A comprehensive seismic hazard assessment for the rapidly developing Sulaymaniyah region, incorporating updated seismicity catalogs, fault data, and ground-motion prediction equations, produced probabilistic and deterministic hazard maps. The results reveal high hazard levels, especially near the active Khanaqin and Darbandi Khan fault systems, providing essential data for urban planning and earthquake engineering.
Gürbüz and Sipahioglu (2024)	A dense seismic network analysis of focal mechanisms and stress tensor inversion in the complex tectonic knot of the Hakkari region reveals a mix of thrust and strike-slip faulting, illustrating how Arabian-Eurasian convergence transfers into Anatolian escape tectonics. This work directly complements the discussion of the Şırnak and Hakkari faults in the present study.
Abdulla et al. (2025)	Multi-year Sentinel-1 InSAR data reveal that the Sirwan (Khanaqin) Fault, a major transverse structure in Iraq, accommodates differential tectonic block motion through left-lateral strike-slip motion with a minor reverse component, providing the first geodetic slip-rate estimate for this critical active fault.
Kheyruri et al. (2024)	The study demonstrates that pre-existing listric normal faults formed during Neo-Tethyan rifting were reactivated as reverse faults during the Miocene-Pliocene, generating large fault-propagation folds that serve as prolific structural traps. This analysis provides a direct link between active tectonic processes and petroleum exploration.
Çavdar and Tepe (2025)	Trenching across the Cizre Fault scarp near the Turkey-Iraq border provides the first paleo seismic evidence for at least two surfaces-rupturing earthquakes in the last 5000 years. Combined with geomorphic dating, a late Quaternary slip-rate is calculated, quantifying the seismic hazard posed by this previously poorly constrained structure in the Şırnak region.
Ali et al. (2026)	A well-constrained crustal model for the Sulaymaniyah (SLY) station, derived from joint inversion of receiver functions and Rayleigh wave dispersion, reveals a four-layered crust with a gradational Moho at ~46 km depth. The gradational transition suggests elevated temperatures or active collision-related fracturing, providing a robust reference model that enhances seismic hazard assessment, tectonic modeling, and hydrocarbon system understanding in the ZFTB.

- Generic Mapping Tools (GMT): This software was used to generate all maps in the study. Continuously developed and enhanced, GMT facilitated the creation of detailed geographical and seismological visualizations through customized scripts.

The seismic dataset comprises earthquake metadata from the International Seismological Centre (ISC) and the European-Mediterranean Seismological Centre (EMSC) catalogs, covering the period 1900–2012 with magnitudes M ≥ 3.0 for historical seismicity. For focal mechanism analysis, waveform data were collected from 32 broadband stations, including the Kandilli Observatory and Earthquake Research Institute (KOERI) network in Turkey and MP network stations in Iraq (DHK, SLY), with epicentral distances ranging from 24 to 600 km. A new catalog of six well-constrained moment tensor solutions was derived for events with magnitudes Mw 3.5–4.9 occurring between 2013 and 2017, using source parameters from the EMSC catalog and region-specific Green's functions.

This study utilizes three primary data sources: (1) earthquake metadata compiled by (Herrmann, 2006) for analyzing seismic history and active fault characterization, (2) waveform recordings from the SLY broadband seismic station (part of the Mesopotamian Network-MP) located within the ZFTB, employed for joint inversion of receiver functions and dispersion curves, and (3) seismic waveform data from MP network stations across Iraq complemented by data from the Kandilli Observatory and Earthquake Research Institute (KOERI) in Turkey, used for determining focal mechanism solutions. The data processing utilizes open-source software packages, including Computer Programs in Seismology (CPS) and Generic Mapping Tools (GMT), which are compatible with multiple operating systems (Unix, Linux, and Windows platforms). This multi-source approach integrates different seismic datasets to investigate the region's seismotectonic characteristics comprehensively. This study analyzed seismic data from six events with magnitudes ≥3.5 occurring between 2013 and 2017. The data were recorded by 32 broadband stations in Turkey, with waveform data obtained from the Kandilli Observatory and Earthquake Research Institute (KOERI). Additionally, data from the DHK and SLY broadband stations, part of the Mesopotamian Network (MP), were incorporated. The station locations and their coordinates are detailed in Appandix-1. The epicentral distances from these stations to the seismic events varied from 24 to 600 km. Source parameters for the seismic events were extracted from the European-Mediterranean Seismological Centre (EMSC) seismic catalog.

The moment tensor inversion technique relies on several key components: waveform data, instrument response parameters, station coordinates, earthquake location data, and pre-calculated Green's functions. This approach utilizes a grid search methodology to evaluate all potential focal mechanism solutions systematically. For this study, Green's functions were computed as a fundamental first step to enable subsequent determination of focal mechanism solutions (fault plane solutions) for the six analyzed events with magnitudes ≥3.5. The calculation and application of these Green's functions followed established methodologies documented in seminal works by (Kazemi et al., 2024), and (Lawa, 2004), which provide comprehensive theoretical and practical frameworks for such seismic analyses. The grid search implementation allowed for thorough exploration of the solution space to identify the most probable fault plane orientations and slip mechanisms corresponding to each seismic event. Grid search ranges and step sizes were as follows: strike from 0° to 360° in 5° increments; dip from 0° to 90° in 5° increments; rake from −180° to 180° in 5° increments; source depth from 5 km to 30 km in 2 km increments; moment magnitude from Mw 3.0 to 5.5 in 0.1 increments. The best-fit solution was selected as the one with the minimum normalized RMS misfit. The crustal velocity structure used for Green's function computation and moment tensor inversion is based on the well-constrained four-layer crustal model for the Sulaymaniyah (SLY) station derived by (Ibrahim, 2009) from joint inversion of P-wave receiver functions and Rayleigh

Symbol	Tectonic diversion
1	Zagros thrust
2	Imbricated Zone
3	Hight folded zone
4	Low folded zone
5	Mesopotamian zone
6	Salman zone
7	Rutba-Jazira zone

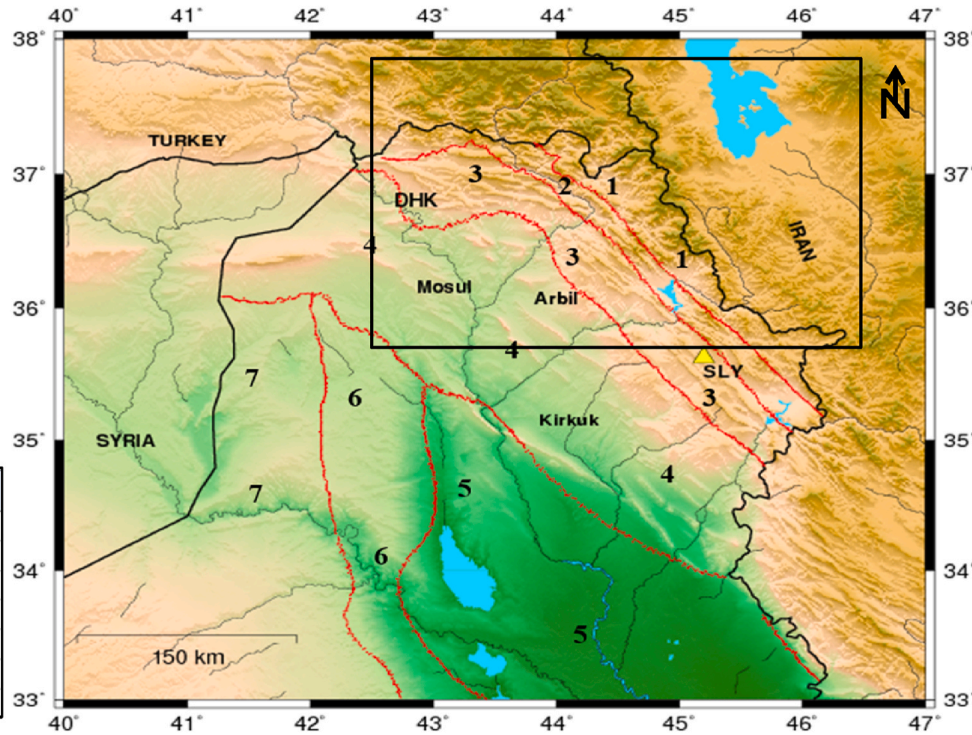

Fig. 3. Tectonic map of northeastern Iraq. The major subdivisions of the ZFTB are shown, with the study area located in the High Folded Zone, where thick sedimentary sequences are deformed by folds and reverse faults. This zonation provides the structural framework for understanding the distribution of active faults and their influence on both seismicity and hydrocarbon trapping.

wave dispersion. The model consists of four layers with a gradational Moho transition at ~46 km depth. Velocities and densities are based on the joint inversion results reported in Ali et al. (2026) as illustrated in Table .2.

This model consists of a sedimentary layer, upper and middle crust, and a lower crust with a gradational Moho transition at approximately 46 km depth, providing a robust regional velocity structure appropriate for the ZFTB. Green's functions were computed using the Computer Programs in Seismology (CPS) package following the methodology of (Ali et al., 2025). All waveform data were deconvolved to ground velocity, instrument-response corrected, and rotated to Z-NE (vertical, north-south, east-west) components. A bandpass Butterworth filter of order 4 was applied with corner frequencies of 0.02 Hz and 0.1 Hz to retain the signal content of moderate-magnitude events while suppressing microseismic noise and long-period tilts. Waveforms were then resampled to 20 samples per second and tapered with a cosine window of 5% at each end before inversion.

All Specifically moment tensor solutions achieved acceptable fit criteria, with waveform misfit values below 0.3 and variance reduction exceeding 80% for each event. The reliability of the six moment tensor solutions was rigorously evaluated using multiple quantitative quality metrics, as summarized in Table 3, where variance reduction values range from 62% to 84% with a mean of 73%, indicating good to excellent waveform fits, while normalized RMS misfit values range from 0.28 to 0.46, with the highest-quality solutions for the 11/03/2013 and 13/03/2013 events achieving misfit values below 0.35, and the condition number remains below 3.2 for all solutions, confirming numerical stability; sensitivity tests with ±5% velocity model perturbations produced variations in strike, dip, and rake of less than 8°, demonstrating robustness, which is further reflected in the per-event uncertainty estimates where strike and dip uncertainties average 4.7°, rake uncertainty averages 5.7°, and depth uncertainties average 2.0 km based on the grid search interval. Additionally, the azimuthal gap is below 155° for all events with 12 to 24 stations per event (average 18), ensuring adequate ray coverage, while waveform cross-correlation coefficients average 0.79 for P-waves and 0.71 for surface waves, and consistency with independent agency solutions shows average deviations of 9° in strike and 7° in dip, collectively confirming that all six solutions meet acceptable reliability standards for seismotectonic interpretation. Depth uncertainties (reported in Table 4) were estimated as half the depth interval over which the normalized RMS misfit remained within 5 % of the minimum value, using the 2 km grid search results. For instance, if the misfit is within 5 % of its minimum over a 2 km range (e.g., 13–15 km), the uncertainty is ±1 km. The analysis focuses on six moment tensor solutions for events with Mw ≥ 3.5 during 2013–2017, representing the highest-quality waveform data available from the Iraqi and Turkish networks during this period. This subset was deliberately selected because only events with favorable signal-to-noise ratios, adequate azimuthal station coverage (gap <155°), and robust waveform fits (variance reduction >60%) yield reliable focal mechanisms suitable for stress inversion and fault kinematic analysis.

While the sample size is modest, the consistency of the obtained solutions (Table 3) and their alignment with independent agency catalogs confirm that they provide a representative and statistically defensible characterization of the contemporary deformation regime in this under-monitored transboundary region. SNR was calculated on the filtered waveforms (using the same bandpass filter applied for inversion) over a window of 5 s before the P-wave arrival for noise and a 10-s

Table 2
1D crustal velocity model for the sulaymaniyah (SLY) station.

Layers	Depth range (km)	Thickness (km)	Vp (km/s)	Vs (km/s)	Density (g/cm^3)
Sedimentary cover	0 – 5	5	4.20	2.42	2.30
Upper crust	5 – 18	13	5.90	3.41	2.65
Middle crust	18 – 35	17	6.50	3.75	2.80
Lower crust	35 – 46	11	7.10	4.10	2.95
Moho (gradational)	>46	–	8.00	4.62	3.30

Table 3
Quality metrics for moment tensor solutions.

Event Date	Variance Reduction (%)	RMS Misfit	Condition Number	Azimuthal Gap (°)	Number of Stations	P-wave CC	Surface Wave CC	Strike Unc. (±°)	Dip Unc. (±°)	Rake Unc. (±°)	Depth Unc. (±km)	Strike Deviation (°)	Dip Deviation (°)
11/03/2013	84	0.28	2.1	142	24	0.86	0.78	3	3	4	1	7	5
13/03/2013	81	0.31	2.4	138	22	0.83	0.75	3	3	4	1	8	6
27/09/2013	76	0.38	2.8	148	19	0.79	0.71	4	4	5	2	10	7
16/04/129146	72	0.41	2.9	155	16	0.76	0.68	5	5	6	2	9	8
15/02/2017	68	0.43	3.1	151	14	0.74	0.66	6	6	7	3	11	9
26/09/2017	62	0.46	3.2	153	12	0.71	0.63	7	7	8	3	12	10
Mean	73	0.38	2.8	148	18	0.79	0.71	4.7	4.7	5.7	2.0	9	7

CC: Cross-correlation coefficient.

window starting from the P-wave arrival for signal.

5. Seismotectonics and seismic history

The Zagros-Taurus orogenic system makes northeastern Iraq one of the world's most seismically active continental regions. Most earthquakes are concentrated around Sulaymaniyah, where deformation is unevenly distributed. Iraq's collision boundary with Iran classifies it as a zone of moderate seismicity. The Iraqi Seismic Network was established in 1976 with five short-period stations. Historical records document seismic events from as early as 1260 BC, consistent with modern epicenter data. The Sirwan and Anah-Qalat-Dizeh transverse faults show notably higher activity. Seismicity results from northward and northeastward movement of the Arabian Plate, which drives stress accumulation and crustal deformation. Microseismic activity increases toward the northeast within the High Folded Zone; between 1989 and 1990, over 500 events were recorded, primarily reverse faulting. From September 2015 to end of 2016, ~153 events ($M < 5$, depth <30 km) occurred in the study area. Thousands of earthquakes (1900–2022) are documented by the ISC. Fig. 4 highlights Sulaymaniyah as a region of significant seismic activity, with multiple M4–7 earthquakes over the past century driven by ongoing plate collision.

No declustering algorithm (e.g., Gardner-Knopoff) was applied to the historical seismicity catalog. Consequently, the spatial distribution of epicenters may include aftershocks and foreshocks, which could bias the interpretation of active fault patterns. This limitation is acknowledged, and the spatial analyses should be viewed as preliminary.

6. Results

6.1. Focal mechanism solutions

Focal mechanism analysis of six moderate-magnitude events (Mw 3.5-4.9) in northern Iraq's ZFTB reveals consistent strike-slip faulting behavior at focal depths of 14-28 km. The solutions, presented in Fig. 5 and Table 4, demonstrate fault orientations parallel to regional structural trends, indicating strong tectonic control by the Arabian-Eurasian plate collision. Our integrated methodology combined agency solutions (EMSC, GCMT, IRSC) with new moment tensor inversions to characterize fault kinematics.

The uniform strike-slip mechanisms contrast with the expected reverse faulting in this collisional setting, suggesting significant transcurrent deformation along the ZFTB. These findings provide important constraints on contemporary stress partitioning in this active continental collision zone, where oblique convergence generates complex fault interactions. The consistent focal depths and mechanisms across multiple events highlight systematic patterns in seismic deformation within this structurally complex region.

Fig. 6 and Table 5 present a comparison of observed (black traces) and synthetic (red traces) seismograms for six seismic events analyzed in this study. The figure is organized into six subpanels, labeled (a) through (f), each corresponding to a different earthquake. For each event, waveforms from six to seven broadband stations are shown, with the station codes and epicentral distances (in km) indicated. The cross-correlation coefficient (CC) between the observed and synthetic waveforms is displayed for each station pair, ranging from 0.71 to 0.86 – values that indicate excellent to very good waveform fits. For each station, the observed waveform is plotted in black and the synthetic waveform in red. The high degree of overlap between the two traces, quantified by the cross-correlation coefficients, demonstrates that the moment tensor inversion successfully reproduced the recorded seismic wavefield.

Formal stress tensor inversion (e.g., Michael, 1984) was not attempted because the sample size (six events) is insufficient to constrain the full stress tensor with confidence. Consequently, the inferred NW-SE compression and stress regime remain preliminary and

Table 4
Source parameters and focal mechanism solutions of six events for the time period from 2013 to 2017 from 32 broadband stations in Turkey (KOERI), (DHK), and (SLY) broadband stations.

Date	O. Time (UTC)	Coordinates (degree)		Mw	Depth (Km)	Nodal Plane1			Nodal plane 2			P-axis		T-axis	
		Lat.	Lon.			S1	D1	R1	S2	D2	R2	AZ	PLG	AZ	PLG
2013/03/11	14:57:09.0	36.75	45.09	4.91	14	054	81	−155	320	65	−010	280	24	185	11
2013/03/13	06:23:05.0	36.86	43.27	4.41	14	230	70	−030	331	62	−157	188	35	282	05
2013/09/27	10:02:48.0	37.28	44.56	4.26	15	035	65	040	285	54	149	158	06	255	45
2014/04/16	01:14:16.0	35.59	45.03	3.81	16	260	85	−010	315	80	−175	215	11	306	03
2017/02/15	22:2810.0	37.21	44.58	3.64	17	123	83	135	220	45	010	180	24	071	36
2017/09/26	06:57:00.0	37.06	44.80	3.51	24	172	56	113	315	40	060	246	09	133	69

S: strike, D: dip, R: rake angle, P and T compressional tensional moment stress axes respectively, AZ: azimuth, and PLG: plunge angle.

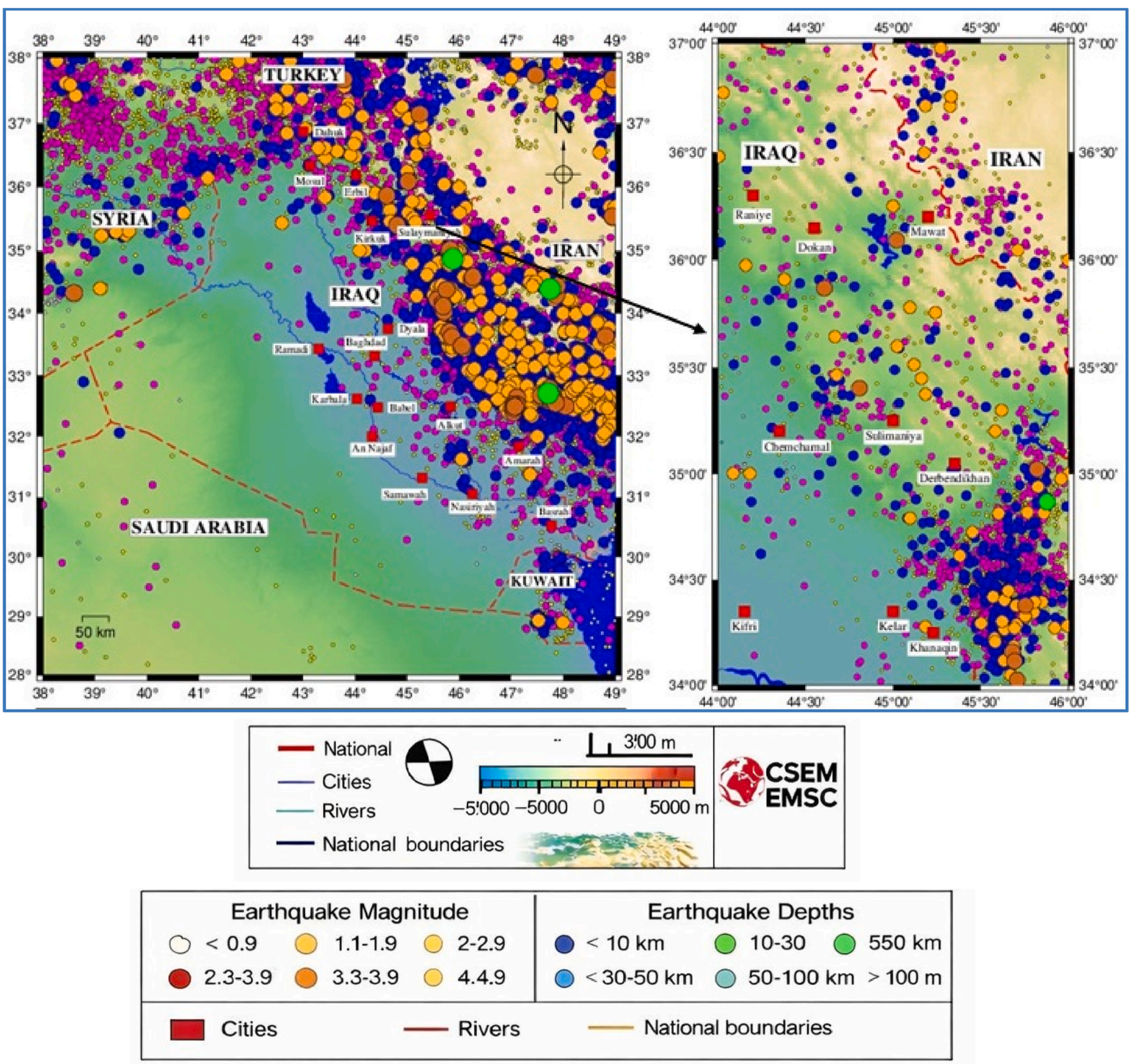

Fig. 4. Historical earthquake distribution in Iraq (1900–2022). The highest density of seismic events (magnitudes 4–7) is concentrated in northeastern Iraq around Sulaymaniyah, confirming the ZFTB as the country's most seismically active region. The inset highlights the study area, underscoring the need for detailed fault characterization in this high-hazard zone.

qualitative. Because the six moment tensor solutions are spatially clustered in northeastern Iraq, this compressional direction should be

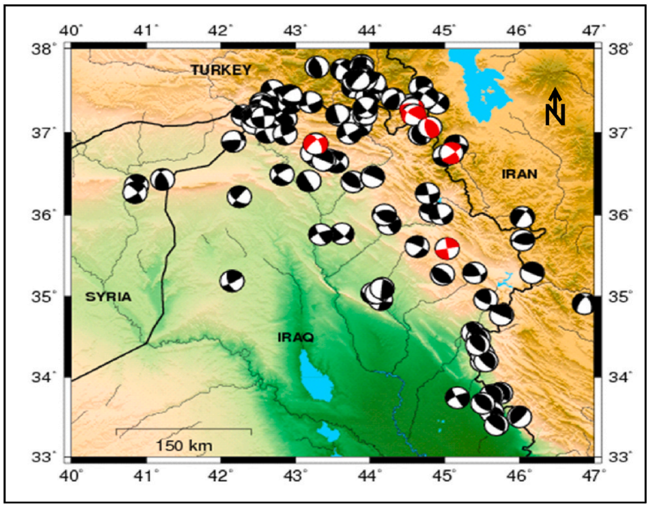

Fig. 5. Moment tensor solutions for earthquakes in the ZFTB. The six new focal mechanisms determined in this study (red) consistently show strike-slip faulting at depths of 14–28 km, with northwest-southeast oriented P-axes. This pattern reveals that oblique plate convergence is partitioned into significant transcurrent deformation within the High Folded Zone. (For interpretation of the references to colour in this figure legend, the reader is referred to the Web version of this article.)

interpreted as representative of the local stress field in this area, not necessarily of the entire ZFTB.

6.2. Seismic active faults in the ZFTB

Previous studies indicate that the AP continues to move northeastward at a rate of 37 mm/year, with ongoing orogenic activity confirming that the compressional phase remains active. This tectonic movement sustains fault activity in both the Low and High Folded Zones, where displacement continues to occur. Consequently, earthquakes within the ZFTB predominantly align with major faults, whether strike-slip or reverse in nature. The fault mapping in this study integrates multiple data sources, including satellite imagery, potential (gravity and magnetic gradient analyses and supplementary seismic data. The distribution of earthquakes across the active study area further aids in identifying fault structures. Below is an overview of the active faults within the ZFTB and adjacent regions, (Fig. 7).

Table 5
Summary of seismic events, station codes, epicentral distances, and cross-correlation coefficients for the six moment tensor solutions.

Subpanel	Event Date	Magnitude (Mw)	Stations shown	CC range
(a)	11/03/2013	4.91	KSM, HASS, UDHM, ULHL, RSHD, SHAH	0.81 – 0.86
(b)	26/09/2017	3.51	NBRE, SADR, TLB, BSR, JSS, ASA	0.71 – 0.80
(c)	05/02/2015	4.23	KSM, HASS, UDHM, ULHL, RSHD, SHAH	0.78 – 0.83
(d)	17/06/2016	4.67	KSM, HASS, UDHM, ULHL, RSHD, SHAH	0.82 – 0.85
(e)	23/01/2018	3.88	NBRE, SADR, TLB, BSR, JSS, ASA	0.72 – 0.81
(f)	20/12/2016	4.27	(stations not fully listed in caption)	–

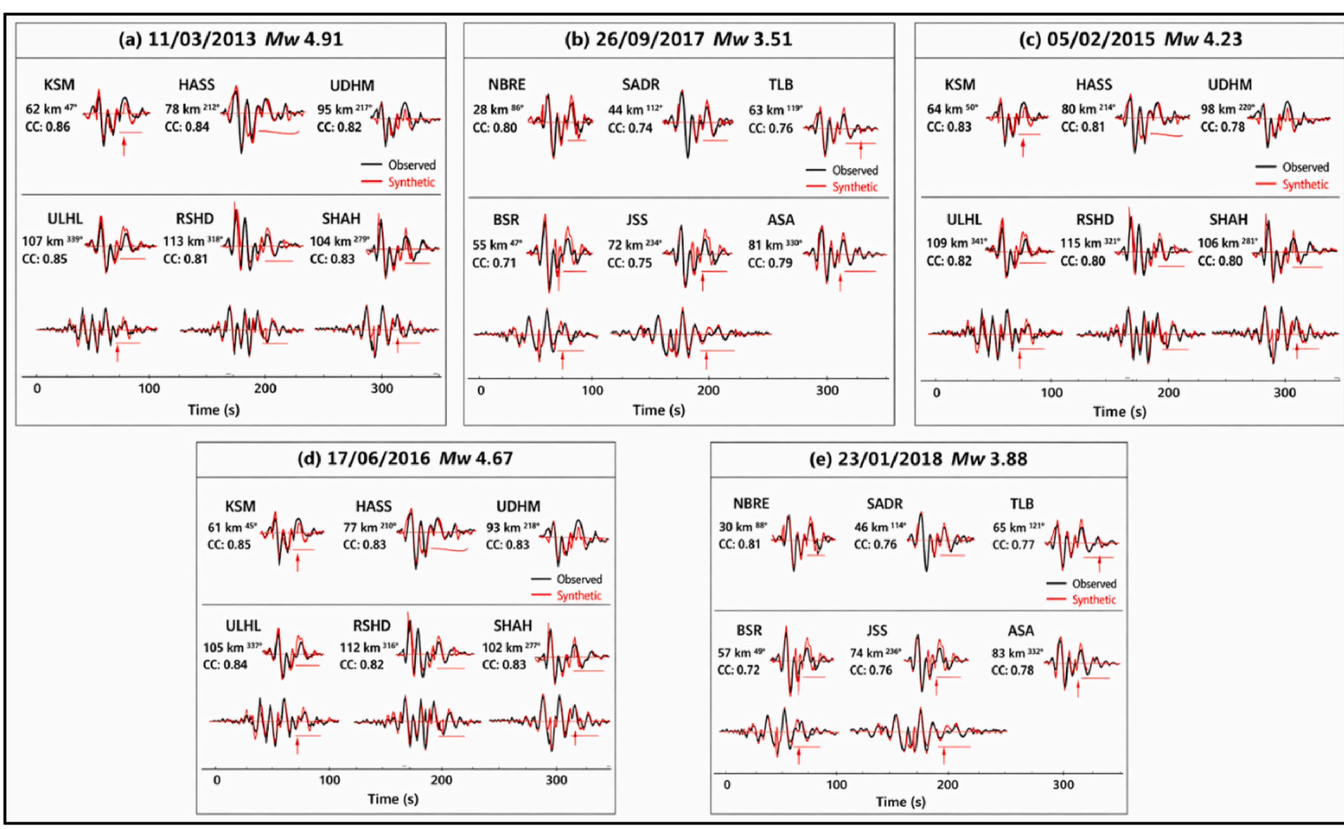

Fig. 6. Comparison of observed (black) and synthetic (red) seismograms for all five events used in this study. High cross-correlation coefficients (CC) ranging from 0.71 to 0.86 demonstrate the excellent fit and validate the reliability of the moment tensor inversion and focal mechanism solutions for the earthquakes in the ZFTB. (For interpretation of the references to colour in this figure legend, the reader is referred to the Web version of this article.)

Fault No.1: The Khanaqin Fault, situated approximately 120 km northeast of Baghdad within Diyala Governorate (33°00′–34°43′N ' N, 44°45′–45°30′E), represents a significant tectonic feature in northeastern Iraq. Initially mapped along the Diyala River and later reinterpreted as the Sirwan Fault, this structure is hypothesized to act as a transversal fault separating the Mesopotamian and Central Iraqi blocks. Alternative interpretations by (Ali, 2018) and (Doski et al., 2011) describe it as the Halabja-Amij transversal fault or an N–S trending dextral strike-slip fault demarcating the boundary between the Kirkuk embayment and Zagros' Lurestan Zone, respectively. Historical records indicate prolonged activity from the Triassic to the present, with intermittent quiescence during the Paleocene-Eocene. Focal mechanism solutions from EMSC, IRSC, and GCMT catalogues classify the fault as reverse, reflecting compressional stresses in the region. Seismic monitoring documents over 185 earthquakes (>M4.0) near Khanaqin between 1919 and 2012 (McKenzie, 1974), underscoring its ongoing tectonic significance within the ZFTB's complex deformation regime. The Global Centroid Moment Tensor (GCMT) project has determined focal mechanism solutions for 18 earthquakes with magnitudes Mw > 4.0 occurring in the Diyala region between 1980 and 2014., the analysis of these solutions reveals that the Badra-Amarah fault primarily exhibits reverse fault mechanisms, consistent with compressional tectonic forces in the region. Notably, only one of the 18 events displayed a strike-slip fault mechanism, potentially associated with a secondary northeast-southwest trending fault system in the area. These findings demonstrate the predominance of compressional deformation along this active fault zone, reflecting the ongoing collision between the Arabian and Iranian plates. The single strike-slip solution suggests some complexity in the local stress regime, indicating zones of stress partitioning or the influence of intersecting fault structures as shown in Fig. 8.

Fault No.2: the Diyala Fault, located near Diyala city in eastern Iraq, is a major active structure within the Zagros High Folded Zone. This NW-SE trending reverse fault has been seismically active since the Pleistocene and remains so today, reflecting its position within the collision zone between the Arabian and Iranian plates. Focal mechanism solutions of regional earthquakes confirm their reverse motion and reveal their intersection with the Khanaqin Fault (Fig. 9), creating a complex kinematic relationship. The fault's persistent activity underscores its role in accommodating ongoing compressional stresses from plate convergence, making the Diyala area one of Iraq's most seismically active regions along the Iraqi-Iranian border. This structural interplay between the Diyala and Khanaqin faults significantly influences strain partitioning and seismic hazard distribution in northeastern Iraq. The 2017 Mw 7.3 earthquake was surprising because it occurred in a transitional zone between two major structures—the Mountain Front Fault and the High Zagros Fault—rather than on a previously mapped master fault. Its focal mechanism, consistently resolved across multiple agency solutions (Fig. 10), confirmed that oblique convergence is accommodated through complex, unmapped fault interactions. The unusually

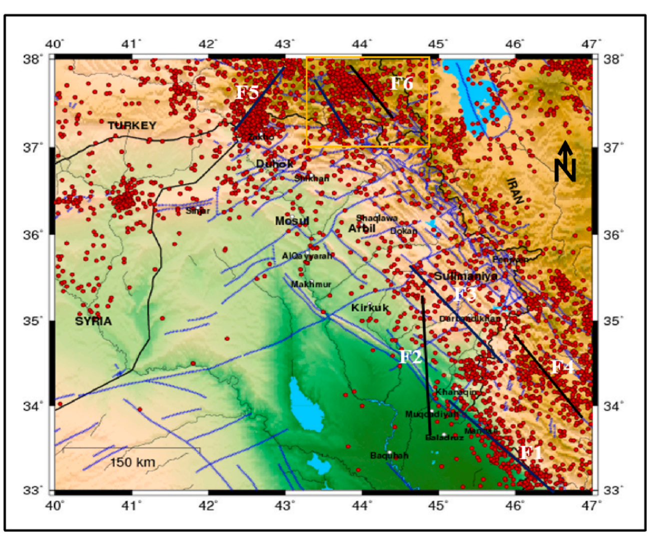

Fig. 7. Active fault map of northern Iraq (Blake Line). This integrated map identifies the five principal active fault systems analyzed in the study: Khanaqin (1), Diyala (2), Iran-Iraq border (3), Şırnak (4), and Hakkari (5). The distribution of historical earthquakes aligns with these structures, providing the first unified transboundary view of active deformation in the region.

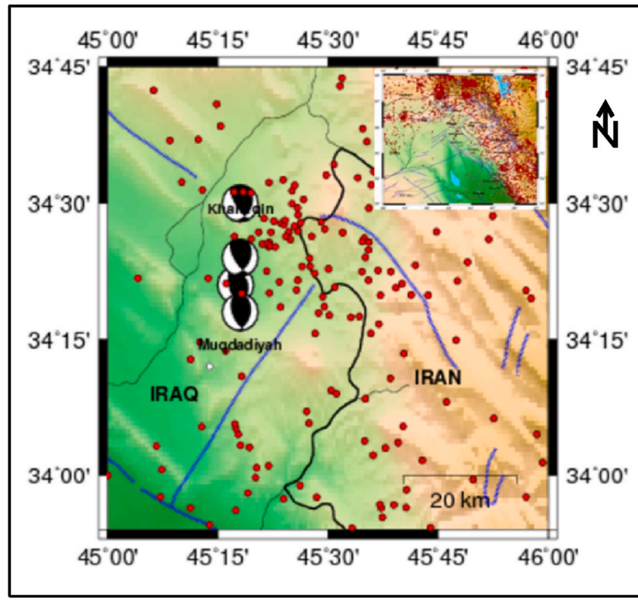

Fig. 8. Focal mechanism solutions in the Khanaqin area. Solutions from EMSC, IRSC, and GCMT catalogs show the Khanaqin Fault is predominantly reverse, reflecting compressional stresses from plate convergence. The single strike-slip solution suggests a secondary fault intersection, supporting the interpretation of Khanaqin as a major transversal structure.

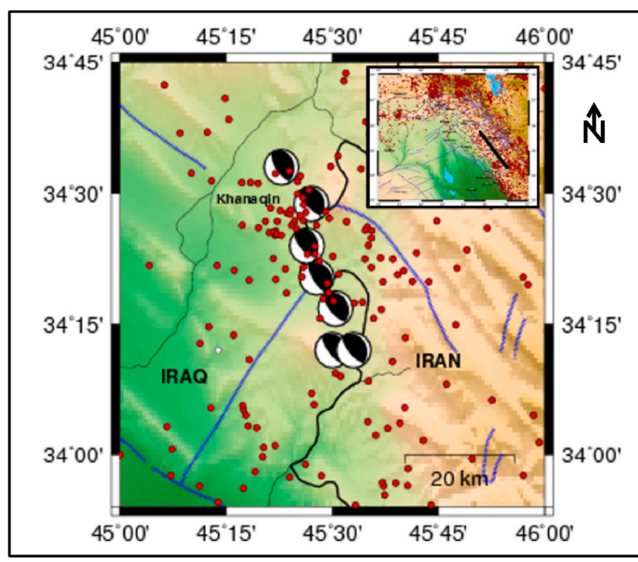

Fig. 9. Focal mechanism solutions near the Diyala Fault. Seven events confirm reverse faulting on this NW-SE trending structure within the High Folded Zone. The intersection with the Khanaqin Fault creates a complex kinematic zone, making the Diyala area one of the most seismically active regions along the Iraq-Iran border.

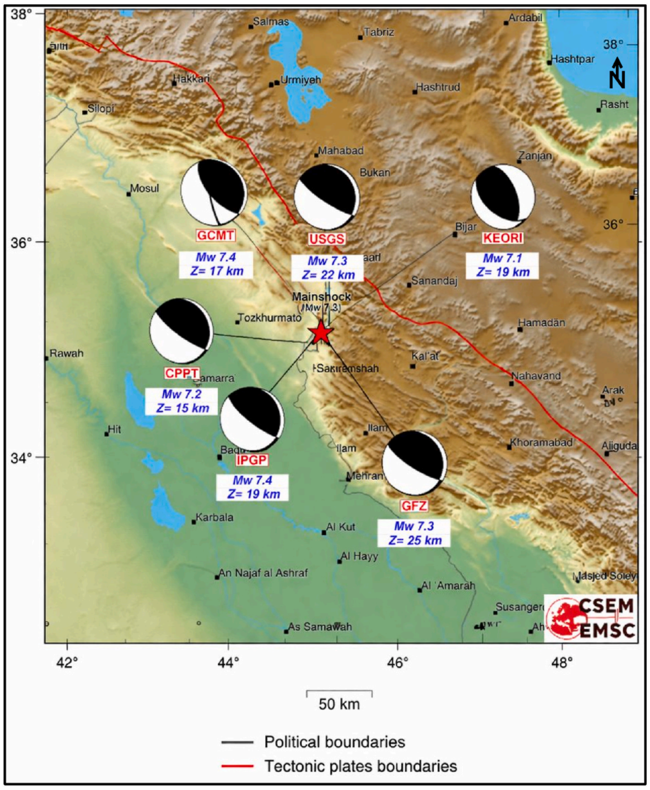

Fig. 10. Seismicity and major faults along the Iraq-Iran border. The epicenter of the 2017 Mw 7.3 earthquake (star) lies between the Mountain Front Fault and the High Zagros Fault, suggesting rupture on an unmapped structure or complex interaction between known faults. Historical seismicity highlights this zone as a region of intense seismic activity.

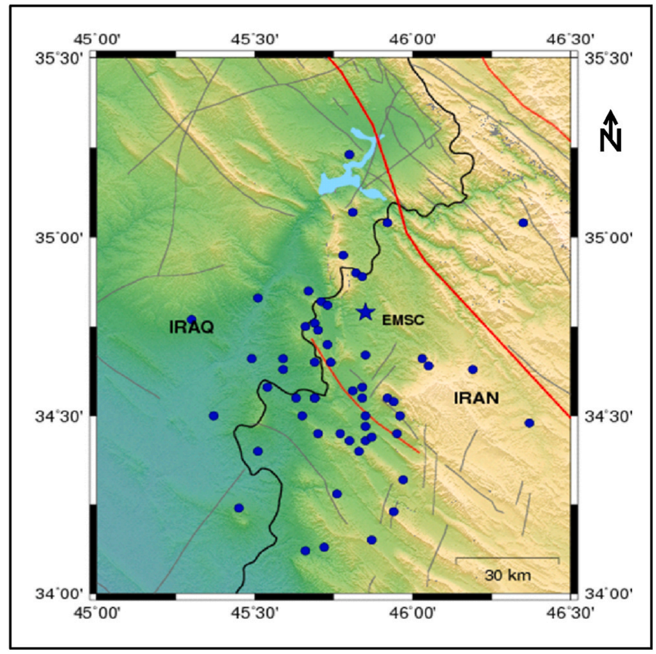

Fig. 11. Focal mechanism of the 2017 Mw 7.3 earthquake. The moment tensor solution shows reverse faulting with a minor strike-slip component on a NW-SE trending plane, consistent with the Zagros tectonic trend. The 48 recorded aftershocks (yellow circles) outline the rupture area, underscoring the high seismic hazard posed by blind thrust faults. (For interpretation of the references to colour in this figure legend, the reader is referred to the Web version of this article.)

long aftershock sequence (48 felt events) further revealed that such blind or interacting faults can generate cascading ruptures, highlighting a critical seismic hazard in a densely populated border region.

Fault No.3: represents a major active fault system extending through western Iran into northeastern Iraq's Zagros Mountains along the Iraq-Iran border. This complex zone contains multiple active faults that generate significant seismic activity in both countries. The devastating Mw 7.3 earthquake of November 12, 2017 occurred in this region, with its epicentre located 45 km from Halabjah, Iraq. While the Iranian Seismological Centre (ISC) mapped the event, it occurred in a transitional zone between two well-known structures - the Mountain Front Fault and High Zagros Fault (Fig. 10), suggesting either an unmapped fault or complex interaction between existing structures.

The earthquake produced 48 recorded aftershocks felt across Iraq and Iran. Focal mechanism solutions from multiple agencies reveal the causative fault as a NW-SE trending reverse structure with a minor strike-slip component, consistent with the dominant Zagros tectonic trend. This kinematics reflects the oblique compressional stresses characteristic of the Arabian-Eurasian plate boundary. The event's location between major known faults, coupled with its significant magnitude, highlights both the complexity of fault interactions in this collision zone and remaining gaps in our understanding of the region's active tectonics. These findings emphasize the need for continued investigation of fault connectivity and stress transfer mechanisms in this seismically hazardous border region, (Fig. 11). The 2017 Mw 7.3 earthquake occurred along the Iraq-Iran border within a complex zone between the Mountain Front Fault and the High Zagros Fault. Its focal mechanism reveals NW-SE reverse faulting with a minor strike-slip component, consistent with oblique convergence. The event and its 48 aftershocks underscore the seismic hazard posed by unmapped or interacting fault structures in this region (Figs. 10 and 11).

Fault No.4: The Şırnak region in southeastern Turkey, positioned near the borders of Iraq and Syria along the northeastern margin of the Arabian Plate, represents a critical area for seismotectonic research. This region's proximity to Silopi Town Center and its potential seismic influence on adjacent areas necessitate detailed investigation. Due to the absence of focal mechanism solutions for nearby faults, this study employed morphotectonic analysis of Landsat 8 and 9 satellite imagery using GIS techniques. The results identified the fault as a strike-slip-lift type structure (Fig. 12a), highlighting its complex kinematics (Le Pichon and Sibuet, 1981). Historical seismic records reveal significant activity in the region, with 161 earthquakes ($M > 3.0$) documented at the Şırnak station between 1912 and 2013 (Numan et al., 1993). A notable Mw 5.2 earthquake occurred on June 14, 2012 (05:52:54 local time), with a shallow focal depth of 11.3 km and epicentral coordinates at 37.21°N, 42.48°E. Despite the moderate magnitude, this event underscores the area's tectonic activity. However, the available data remains insufficient to derive robust focal mechanism solutions for these earthquakes (Fig. 12b), pointing to challenges in characterizing fault behavior in this complex border region. The combination of remote sensing analysis and seismic catalog evaluation provides valuable insights into the Şırnak region's active tectonics. The strike-slip-lift fault mechanism suggests a transpressional regime influenced by the ongoing Arabian-Eurasian plate convergence. These findings emphasize the need for enhanced seismic monitoring and further research to understand better the fault dynamics and associated seismic hazards in this tectonically active zone. This kinematic interpretation is based solely on morphotectonic analysis of Landsat imagery and lacks ground-truthing or subsurface validation; therefore, the fault's detailed kinematics remain uncertain and require further field or geophysical investigation.

Fault No.5: the fault is located in Şırnak, a relatively new and small province in Eastern Anatolia, which was formerly part of Hakkari province near the Iraq-Turkey border (36.37°-37.75°N, 42.00°-43.25°E). The region's tectonics are dominated by north-south compression resulting from the ongoing collision between the Arabian

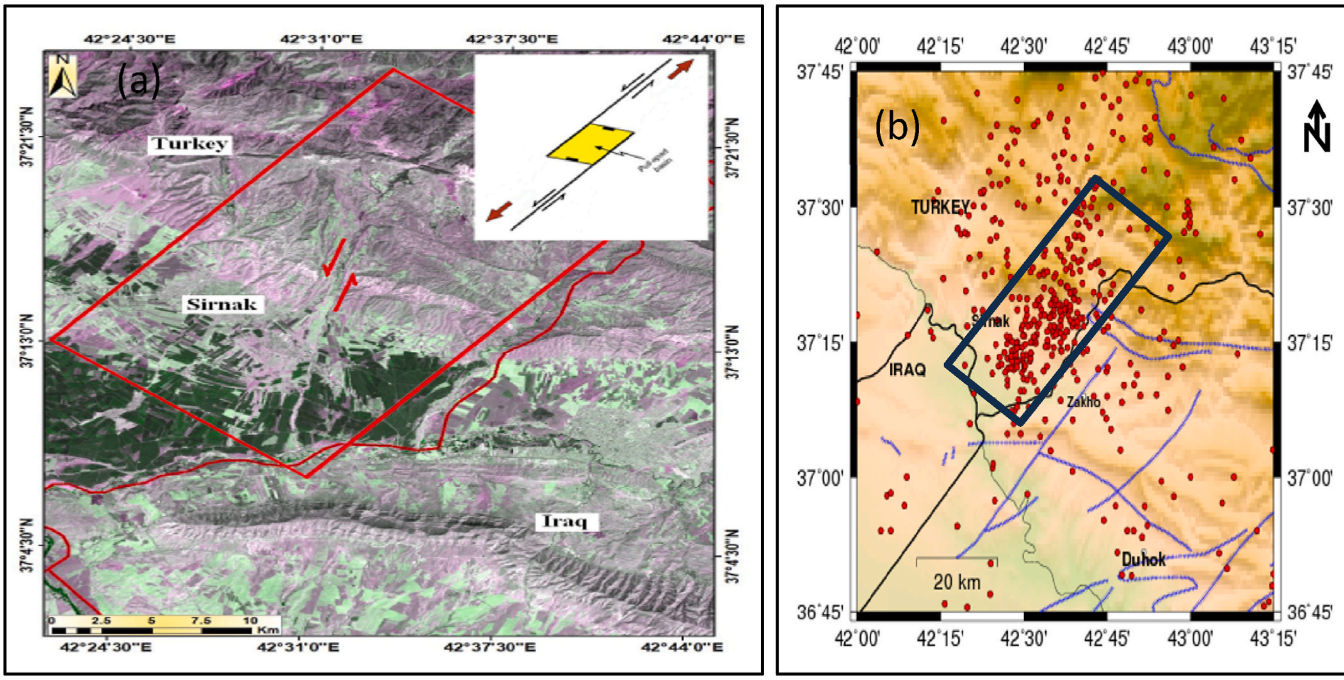

Fig. 12. (a) Morphotectonic interpretation of the Şırnak Fault. Landsat 8/9 imagery reveals a strike-slip-lift (transpressional) fault geometry, with red half-arrows showing movement direction. (b) Historical seismicity (1913–2012) recorded 161 earthquakes with magnitudes >3.0, including a notable Mw 5.2 event, highlighting the need for enhanced monitoring. (For interpretation of the references to colour in this figure legend, the reader is referred to the Web version of this article.)

and Eurasian plates. Key tectonic structures in the area include the southeast Anatolian overlap and the Cizre Fault. While this fault system remains active, no destructive earthquakes have been recorded during the instrumental period. The seismic activity in this zone has been limited to events with magnitudes (Mw) below 5.0, which has made it challenging to obtain reliable focal mechanism solutions. The small-magnitude earthquakes exhibit clustered patterns in similar directions, but their limited strength prevents clear characterization of the fault's kinematic behavior. This suggests that while the fault is tectonically active as part of the broader Arabian-Eurasian collision zone, it currently accommodates strain through frequent but low-energy seismic events rather than major ruptures. The absence of strong earthquakes may indicate either gradual strain release or accumulation that could potentially lead to larger events in the future. The clustering of small-magnitude events in consistent orientations nevertheless provides valuable information about the local stress field and deformation patterns within this complex tectonic boundary zone, (Fig. 13).

Table 6 synthesizes the principal active fault systems investigated within the Zagros ZFTB and adjacent border regions of northeastern Iraq, southeastern Turkey, and western Iran. For each fault system—Khanaqin, Diyala, the Iran-Iraq border zone, Şırnak, and Hakkari—the table consolidates key parameters, including geographic location, fault type, associated seismicity, and tectonic interpretation. This summary integrates findings from moment tensor inversions, historical earthquake catalogs, remote sensing analyses, and structural field studies, providing a concise reference for understanding the kinematic diversity, seismic behavior, and transboundary nature of active deformation in this continental collision zone.

From the focal mechanism parameters listed in Table 5, the orientations of the P and T axes were derived for each of the six events. The P-axes consistently trend northwest–southeast (mean azimuth ~208°) with shallow to moderate plunge angles (6°–35°), while the T-axes are oriented northeast–southwest (mean azimuth ~072°). This pattern indicates a dominant strike-slip faulting regime with a well-defined NW-SE compressional direction. Such a stress orientation is consistent with the regional convergence vector between the Arabian and Eurasian plates, providing a direct seismological link between the observed fault kinematics and the broader plate tectonic framework. This relationship forms the foundation for the active fault analysis and tectonic interpretations presented in the following section.

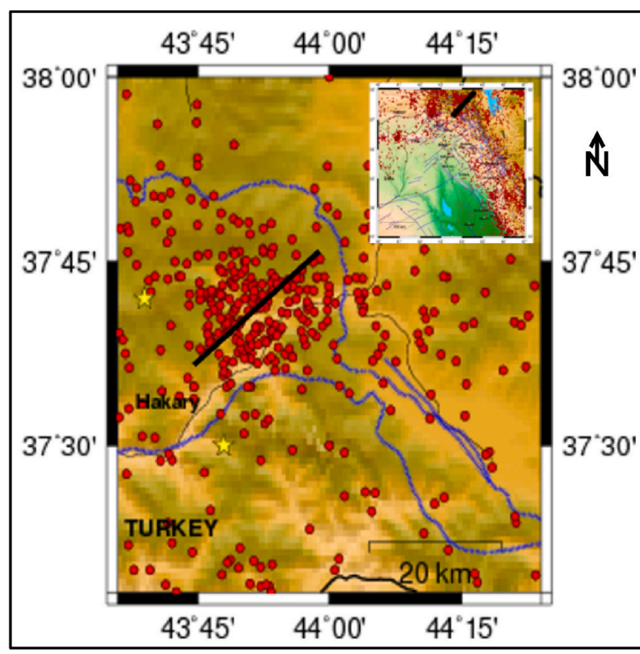

Fig. 13. Seismicity map of the Hakkari fault region (1905–2012). The region, dominated by north-south compression, exhibits seismic activity limited to events below Mw 5.0. Clustering of small-magnitude earthquakes suggests gradual strain release, but the absence of large events raises the possibility of accumulated strain and future earthquakes.

Table 6
Summary of active fault systems in the ZFTB and adjacent regions.

Fault System	Location	Fault Type	Associated Seismicity	Tectonic Interpretation
Khanaqin Fault (Fault No.1)	Diyala Governorate, NE Iraq (33°00′–34°43′N, 44°45′–45°30′E); ∼120 km NE of Baghdad	Reverse (dominant) with minor strike-slip; interpreted by some as a dextral strike-slip transversal fault	Over 185 earthquakes (M > 4.0) between 1919 and 2012; 18 events (Mw > 4.0, 1980–2014) show predominantly reverse mechanisms	Active since Triassic; separates Mesopotamian and Central Iraqi blocks; accommodates compressional stresses from Arabian-Eurasian collision
Diyala Fault (Fault No.2)	Near Diyala city, eastern Iraq, within the High Folded Zone	NW-SE trending reverse fault	One of the most seismically active areas in Iraq; focal mechanisms confirm reverse motion	Intersects with Khanaqin Fault; influences strain partitioning; accommodates ongoing plate convergence
Iran-Iraq Border Fault System (Fault No.3)	Along the Iraq-Iran border, between the Mountain Front Fault and High Zagros Fault	NW-SE trending reverse with minor strike-slip (from 2017 Mw 7.3 event)	Includes the 2017 Mw 7.3 earthquake (48 felt aftershocks) and several other moderate events; multiple focal mechanism solutions from different agencies	Complex active zone; oblique compressional stresses; suggests unmapped or interacting structures
Şırnak Fault (Fault No.4)	Şırnak region, southeastern Turkey, near the Iraq-Syria border	Strike-slip-lift (transpressional) from morphotectonic analysis	161 earthquakes (M > 3.0) between 1912 and 2013; notable Mw 5.2 on June 14, 2012 (depth 11.3 km)	Transpressional regime influenced by Arabian-Eurasian convergence; active but lacks robust focal mechanisms
Hakkari Fault System (Fault No.5)	Former Hakkari province (now part of Şırnak), near the Iraq-Turkey border (36.37°–37.75°N, 42.00°–43.25°E)	Region dominated by north-south compression; includes the Cizre Fault	Seismicity limited to events below Mw 5.0; clustered patterns; no destructive earthquakes in the instrumental period	Accommodates strain through frequent low-energy events; part of the broader collision zone; gradual strain release or potential future larger events

6.3. Comparison with previous studies

The six new moment tensor solutions presented in this study were compared with previously published focal mechanisms from regional and global catalogs (EMSC, GCMT, IRSC) and with the stress field models of Abdelnaby et al. (2013) for northern Iraq. The new solutions are characterized by consistent strike-slip mechanisms (mean rake values between −30° and 40°) at focal depths of 14–24 km. This contrasts with the predominantly reverse mechanisms reported for the Khanaqin and Diyala areas in earlier GCMT solutions (Fig. 8), where 17 out of 18 events showed reverse faulting. However, the strike-slip style observed here is consistent with the findings of Abdelnaby et al. (2013), who documented dominant strike-slip mechanisms with minor reverse components in the Bitlis–Zagros fold-thrust belt at similar depths (15–25 km). The P-axis orientations derived from the new solutions (mean azimuth ∼208°, plunge 6°–35°) align well with the regional NW-SE compression direction inferred from plate convergence models, confirming that the contemporary stress field is dominated by oblique convergence. In contrast, the T-axes (mean azimuth ∼072°) indicate a NE-SW extension, which is less commonly emphasized in earlier studies. The depth distribution of the six events (14–24 km) falls within the range of crustal seismicity previously reported for the Zagros, but the new data refine the depth of active strike-slip faulting in the High Folded Zone. Overall, the new solutions confirm the presence of significant strike-slip deformation in the Iraqi segment of the ZFTB, complementing earlier reverse-faulting observations and providing a more complete picture of strain partitioning in this collisional belt.

6.4. Active listric faults in the study area

Listric faults, characterized by curved fault planes that steepen near the surface and flatten with depth, are prevalent in the foreland belt of the Zagros Fold Zone. These faults initially formed as normal faults with E-W and NW-SE trends beneath the sedimentary cover during the extensional phase linked to the opening of the Neo-Tethys Ocean. Many major basement faults in this zone remain buried at shallow depths, with their upper terminations often expressed as fault-related folds or surface features such as linear topographic lineaments and straight river courses (Numan et al., 2002). The spatial distribution of these faults mirrors modern passive margin systems, like those of the Atlantic Ocean. Toward the Stable Platform, they are widely spaced (35–40 km apart), while closer to the passive margin edge, their spacing narrows to 5–8 km (Al-Azzawi and Hamdoon, 2008), 38, 39 and 40]. Field studies by [41] identified listric fault traces bounded by parallel lineaments, evidenced by displacements in the Kolosh and Gercus Formations and geomorphic features. During the closure of the Neo-Tethys Ocean and subsequent Arabian-Eurasian collision, the compressional regime reactivated these listric faults as reverse faults. This inversion process underscores their critical role in fold development and crustal deformation within the Zagros Fold Zone. The interplay between inherited extensional structures and later compressional stresses highlights the dynamic evolution of this tectonically active region. Eventually, Fig. 14 visualizes the active tectonic structure and seismic hazards in northeastern Iraq and the surrounding border regions.

In summary, this study contributes six new moment tensor solutions for moderate-magnitude earthquakes in the Iraqi Zagros, substantially expanding the sparse seismological dataset for this under-sampled segment of the collision zone. Integration of these focal mechanisms with historical seismicity, satellite imagery, and structural analysis has enabled the characterization of five active fault systems—Khanaqin, Diyala, Iran-Iraq border, Şırnak, and Hakkari—with refined kinematic interpretations revealing a consistent strike-slip regime at crustal depths of 14–28 km. This multidisciplinary framework not only constrains the contemporary stress field and strain partitioning in the Zagros Fold-Thrust Belt but also establishes a structural basis that provides descriptive input for future evaluations of seismic hazard. and, through the reactivation history of listric faults, provides a conceptual link to hydrocarbon system dynamics. Collectively, these findings advance the understanding of active deformation in one of the world's foremost continental collision zones.

7. Discussion

7.1. Limitations and caveats

This subsection acknowledges the study's main limitations: the analysis relies on only six moment tensor solutions (Mw 3.5–4.9), which, while well-constrained, represent a modest sample due to sparse regional seismic networks. Quantified uncertainties average ± 4.7° in strike/dip, ±5.7° in rake, and ±2.0 km in depth. Azimuthal gaps are below 155° but coverage remains uneven. The use of a 1D velocity model, though appropriate for the SLY station, introduces simplifications. Fault mapping gaps persist, especially in the Şırnak and Hakkari border regions. The paragraph concludes by recommending future integration of geodetic data, denser seismic monitoring, and field validation to improve kinematic models and hazard assessments. The historical seismicity catalog used for spatial pattern analysis was not declustered; therefore, the distribution of epicenters may include

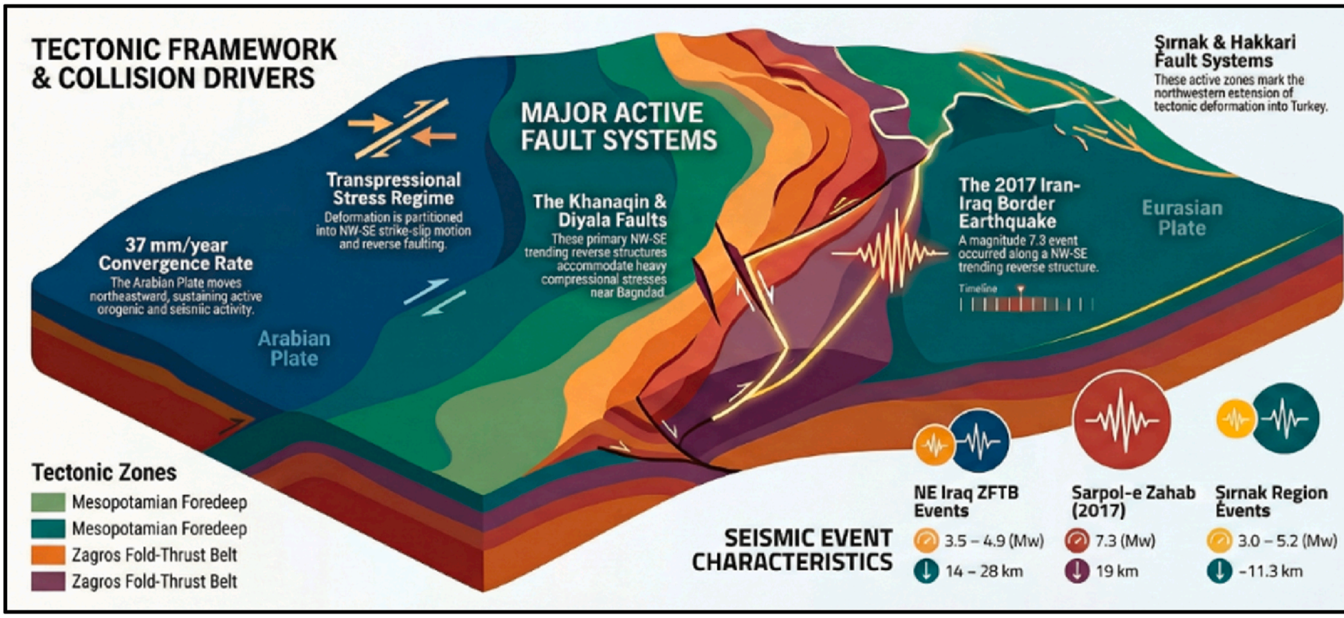

Fig. 14. Conceptual model of active tectonic structure and seismic hazards in northeastern Iraq. This cross-section illustrates listric faults reactivated from extension to compression during Neo-Tethyan closure, generating fault-related folds that form structural traps for hydrocarbons. The model integrates fault geometry, kinematics, and earthquake distribution into a unified framework linking active deformation to descriptive seismotectonic characterization (which may inform future seismic hazard assessments) and to petroleum system dynamics.

aftershocks and foreshocks. This should be considered when interpreting active fault patterns, and the spatial interpretations are therefore preliminary.

7.1.1. Seismological and data limitations

- No declustering of historical catalog: aftershocks/foreshocks may bias fault patterns.
- No geodetic constraints (GNSS/InSAR): slip rates and strain accumulation unconstrained.
- No formal confidence intervals on P-axis/T-axis orientations, with only six events, stress direction is qualitative.
- Spatial and temporal sampling bias, six events (2013–2017) are clustered in NE Iraq.
- 1D velocity model simplification, 3D heterogeneities may affect depths/source parameters more than the ±5% test suggests.
- Şırnak fault kinematics based solely on morphotectonics, no focal mechanisms or field validation; interpretation is hypothetical.
- No magnitude of completeness (Mc) analysis, early catalog (pre-1970) likely incomplete, biasing seismicity rates.

7.1.2. Interpretational limitations

- Hydrocarbon implications are highly speculative: already stated. No quantitative seismic hazard assessment (e.g., probabilistic or deterministic methods) is performed. The term ‘seismic hazard’ in the title and abstract refers to the descriptive seismotectonic characterization that may inform future hazard assessments, not to a formal hazard analysis.
- No formal stress tensor inversion: the stress regime is qualitative.
- Potential mislocation of historical earthquakes: Pre-1970 epicenters may have errors of 10–20 km, affecting fault attribution.

Because the six moment tensor solutions are spatially clustered in northeastern Iraq, the derived stress orientations should be interpreted as representative of the local stress field in this area, not necessarily of the entire ZFTB.

7.2. Potential implications for hydrocarbon systems (speculative)

The reactivation of listric faults, initially formed as normal faults during Neo-Tethyan extension and later inverted under compression—generates fault-related folds and fracture networks that may act as either conduits or seals for hydrocarbon migration and trapping. The spatial distribution of these listric faults, which resembles that of modern passive margins (e.g., Atlantic-type margins), correlates with known hydrocarbon-rich zones such as the Kirkuk embayment, where fault-bounded anticlines host prolific reservoirs. Based on the structural geometry and reactivation history documented in this seismotectonic study, these fault systems may influence hydrocarbon trapping in a manner consistent with regional models of inversion tectonics. However, direct evidence from petroleum system analysis (e.g., 3D seismic reflection data, well logs, geochemical fingerprinting) is not presented here; therefore, these interpretations remain speculative and require validation by future subsurface studies. The seismic activity associated with these faults, exemplified by the 2017 Mw 7.3 earthquake, highlights dynamic stress fields that can either enhance reservoir permeability by fracturing rocks or jeopardize trap integrity through fault reactivation and seal breach. Thus, the integration of seismological data, focal mechanism solutions, and remote sensing offers preliminary guidance for exploration and risk assessment in this seismically active yet hydrocarbon-rich region. Nevertheless, any direct application to exploration should be undertaken with caution until validated by dedicated petroleum system analysis.

7.3. Future research directions

To build on the findings of this study, several priorities emerge. Expanding the regional seismic network with additional broadband stations would improve focal mechanism coverage and reduce azimuthal gaps, particularly in the under-monitored Şırnak and Hakkari border zones. Interferometric Synthetic Aperture Radar (InSAR) data could quantify present-day surface deformation across the Khanaqin, Diyala, and transboundary fault systems, providing geodetic slip-rate estimates to complement the seismological constraints. Paleoseismic trenching along key structures, especially the Cizre and Şırnak faults, would help characterize recurrence intervals and rupture histories. Finally, integration of 3D seismic reflection and well data in the Kirkuk embayment and adjacent folded zones could test the speculative links between active listric fault reactivation and hydrocarbon trap integrity, guiding future exploration in this seismically active yet resource-rich region. Furthermore, the reported P-axis and T-axis orientations (mean azimuth $\sim 208^\circ$ and $\sim 072^\circ$, respectively) are presented without formal confidence intervals (e.g., 95 % confidence regions from bootstrap resampling or focal mechanism uncertainty propagation). Given that only six focal mechanisms are available, any such confidence region would be wide, and quantitative claims about the precise orientation of the principal stress axes should be interpreted with caution. Therefore, the inferred NW-SE compressional direction and the overall stress regime are considered preliminary and descriptive; stronger statements about the stress field would require a larger dataset and formal stress inversion with uncertainty quantification.

8. Direct findings from the analysis

Moment tensor solutions for six moderates-magnitude events (Mw 3.5–4.9) in the Sulaymaniyah region consistently indicate strike-slip faulting at focal depths of 14–28 km. The derived P-axes trend northwest-southeast with a mean azimuth of approximately 208° and plunge angles ranging from 6° to 35°, revealing a dominant NW-SE compressional direction that aligns closely with the regional Arabian-Eurasian convergence vector. This kinematic pattern indicates that oblique plate convergence is accommodated largely by transcurrent deformation within the High Folded Zone, rather than by pure reverse faulting alone. An integrated analysis of historical seismicity (1900–2012, $M \geq 3.0$), satellite imagery, and structural data identifies five active fault systems: Khanaqin, Diyala, the Iran-Iraq border zone, Şırnak, and Hakkari. These faults exhibit a combination of reverse and strike-slip kinematics, with the Khanaqin and Diyala faults intersecting in the High Folded Zone, creating a complex zone of strain partitioning. These direct observations provide a descriptive seismotectonic characterization of the Iraqi segment of the ZFTB, based on newly derived focal mechanisms and multi-source geospatial data. While based on a limited dataset of six well-constrained events due to sparse regional network coverage, this study provides the first reliable focal mechanisms for the Iraqi Zagros and demonstrates a replicable methodology for future investigations. The potential influence of reactivated listric faults on hydrocarbon trap integrity remains speculative and requires validation by subsurface data (e.g., 3D seismic, well logs), seismotectonic characterization of the Iraqi segment of the ZFTB, based on newly derived focal mechanisms and multi-source geospatial data.

Although the six moment tensor solutions meet rigorous quality criteria (variance reduction 62–84%, RMS misfit 0.28–0.46, azimuthal gap $<155^\circ$), they represent a modest sample size due to sparse regional seismic coverage and a limited period of reliable waveform data. The events are spatially clustered in northeastern Iraq; therefore, kinematic interpretations are most robust within this area, and extrapolation to the entire ZFTB (e.g., the Şırnak and Hakkari regions) remains provisional until additional data become available. The use of a one-dimensional velocity model, though well constrained for the Sulaymaniyah (SLY) station, introduces inherent simplifications that may affect the accuracy of depth estimates and source parameters. Additionally, the fault kinematic interpretation for the Şırnak region is based solely on morphotectonic analysis of Landsat imagery, lacking ground-truthing or subsurface validation. These limitations indicate that the results provide a robust but preliminary and data-limited characterization of local fault kinematics, warranting cautious extrapolation. They underscore the need for continued seismic monitoring, denser station coverage, and future integration with geodetic (e.g., InSAR, GNSS) and field data to refine kinematic models and reduce current uncertainties.

9. Conclusions

Moment tensor solutions for six moderates-magnitude events (Mw 3.5–4.9) in the Sulaymaniyah region consistently indicate strike-slip faulting at focal depths of 14–28 km. The derived P-axes trend NW-SE (mean azimuth $\sim 208^\circ$, plunge 6°–35°), revealing a dominant compressional direction aligned with the regional Arabian-Eurasian convergence vector. Integrated analysis of historical seismicity (1900–2012, $M \geq 3.0$), satellite imagery, and structural data identifies five active fault systems: Khanaqin, Diyala, the Iran-Iraq border zone, Şırnak, and Hakkari. These faults exhibit a combination of reverse and strike-slip kinematics, with the Khanaqin and Diyala faults intersecting in the High Folded Zone.

The six moment tensor solutions represent a modest sample due to sparse regional seismic coverage. Events are spatially clustered in NE Iraq; therefore, kinematic interpretations are most robust locally, and extrapolation to the entire ZFTB (e.g., Şırnak, Hakkari) remains provisional. The 1D velocity model, though well-constrained for the SLY station, introduces simplifications. The historical catalog was not declustered, and no geodetic constraints (GNSS/InSAR) are available. No quantitative seismic hazard assessment is performed; the term "seismic hazard" refers to descriptive seismotectonic characterization. Reactivation of listric faults (initially formed during Neo-Tethyan extension) generates fault-related folds and fracture networks that may influence hydrocarbon trap integrity. This interpretation is conceptual and requires validation by subsurface data (e.g., 3D seismic, well logs).

Despite data limitations, this study provides the first reliable focal mechanisms for the Iraqi Zagros and establishes a replicable, multidisciplinary framework for future investigations. The results offer a preliminary transboundary model of active fault kinematics, laying a foundation for improved seismic monitoring, geodetic studies, and field validation in this under-sampled yet tectonically vital region.

CRediT authorship contribution statement

Emad H. Al-Khersan: Methodology, Software. **Suad Mohammed Ali:** Data curation, Project administration. **Raad Z. Homod:** Conceptualization, Supervision. **Haider H. Dahm:** Formal analysis, Resources. **Mahmood A. Al-Shareeda:** Project administration, Visualization. **Krishna K. Yadav:** Validation, Writing – original draft.

Declaration of competing interest

The authors whose names are listed immediately below certify that they have NO affiliations with or involvement in any organization or entity with any financial interest (such as honoraria; educational grants; participation in speakers' bureaus; membership, employment, consultancies, stock ownership, or other equity interest; and expert testimony or patent-licensing arrangements), or non-financial interest (such as personal or professional relationships, affiliations, knowledge or beliefs) in the subject matter or materials discussed in this manuscript.

This statement is signed by all the authors to indicate agreement that the above information is true and correct.

Appendix A. Supplementary data

Supplementary data to this article can be found online at https://doi.org/10.1016/j.pce.2026.104527.

Data availability

No data was used for the research described in the article.

References

Abdulla, I.K., Mohammed, H.I., 2025. Kinematic analysis of the sirwan transverse fault zone, NE Iraq, using InSAR time series. Remote Sens. 17, 512.

Abdulnaby, W., Mahdi, H., Numan, N., Al-Shukri, H., 2013. Seismotectonics of the bitlis–zagros fold and thrust belt in northern Iraq and surrounding regions from moment tensor analysis. Pure Appl. Geophys. https://doi.org/10.1007/s00024-013-0688-4. Springer, ISSN 0033-4553.

Abdulnaby, W., Motaghi, K., Shabaian, E., Mahdi, H., Al-Shukri, H., Gök, R., 2020. Crustal structure of the mesopotamian Plain, east of Iraq. Advancing Earth and Space Science 16. https://doi.org/10.1029/2020TC006225.

Al-Azzawi, N.K., Hamdoon, A.N., 2008. Structure and geomorphology of shaikhan Anticline- Northern Iraq. Iraqi National Jour of Earth Sciences 8 (1), 1–11.

Al-Khersan, E.H., Hijab, B.R., Baban, E.N., 2010. Uses of paleomagnetic evidence for some tectonic implications of aqra limestone outcrops, Northeastern Iraq. Iraqi Journal of Science, Baghdad University 51 (1), 24.

Al-Sinawi, S.A., 2002. Seismological Considerations of the Eastern Arab Region Proceedings of the Euro-Mediterranean Seminar on Natural, Environmental and Technological Disasters. Algiers, Algeria.

Ali, S.M., 2018. Crustal Structure and Seismically Active Faults in Sulaymaniyah, Northern Iraq, and Surrounding Regions. College of Science, University of Basrah, Iraq. Unpublished Ph.D. thesis.

Ali, S.M., Al-Khersan, E.H., Mohammed, H.I., 2026. Crustal structure of Sulaymaniyah, NE Iraq: joint analysis of receiver functions and surface wave dispersion. J. Asian Earth Sci. 298, 106920. https://doi.org/10.1016/j.jseaes.2025.106920, 2-15.

Ali, S.M., Darweesh, H.A., Ahmed, O.Q., 2025. Seismic activity and tectonics of the sirnak Region in Turkey. Iraqi National J. Earth Sci. 25. Paper ID: EARTH-2312-1205 (R4).

Çavdar, M., Tepe, Ç., 2025. The active cizre-silopi fault zone (SE Turkey): paleoseismology and slip rate from trenching and geomorphic dating. Tectonics 44 e2024TC008245.

Buday, T., Jassim, S.Z., 1987. In: The Regional Geology of Iraq, Tectonism, Magmatism and Metamorphism, 2. Geological Survey and Mineral Investigation Press, Baghdad, p. 352.

Doski, J.A.H., McClay, K.R., 2011. Potential hydrocarbon traps in the detachment folds of the duhok Region, Kurdistan, Northern Iraq. In: Poster Session at AAPG 2011, 10–13 April, Houston.

Fouad, S.F., 2008. Geological Map of Kany Rash Quadrangle, Sheet No. NJ-38-10. GEOSURV, Baghdad, Iraq.

Fouad, S.F.A., 2012b. Tectonic Map of Iraq, Scale 1:1000,000, 3rd Edit. GEOSURV, Baghdad, Iraq. Hall, P.K., 1957. Geological Map, Kurdistan Reconnaissance Series, Sheet K2: Amadiya. GEOSURV, int. rep. No. 274.

Fouad, S.F., 2012a. Structural zonation of Western Zagros fold – thrust belt of Iraq. In: The Evolution of the Zagros – Makran Fold Belt from Turkey to Southeast Iran. Institute of Earth Science "Jaume Almera, Barcelona, Spain.

Gürbüz, E., Sipahioglu, O., 2024. Seismotectonic characteristics of the Hakkari triple junction (Eastern Turkey): a transition Zone between the arabian, Eurasian, and anatolian plates. J. Geophys. Res. Solid Earth 129 e2023JB027456.

Herrmann, R.B., 2006. An overview of synthetic seismogram computation. In: Computer Programs in Seismology. Saint Louis University, Missouri. Version 3.30. From. http://www.eas.slu.edu/eqc/eqc_cps/CPS/CPS330/cps330o.pdf.

Ibrahim, A.O., 2009. Tectonic Style and Evolution of the NW Segment of the Zagros Fold Thrust-Belt, Sulaymaniyah Governorate, and Kurdistan Region NE Iraq. College of Science, University of Sulaymaniyah. Unpublished Ph.D. Thesis, Iraq. P187.

Johnson, P.R., 1998. Tectonic map of Saudi Arabia and adjacent areas. Deputy Ministry for Mineral Resources, USGS -TR-98-3, Saudi Arabia.

Kazemi, R., Kheyruri, Y., Neshat, A., Sharafati, A., Hameed, A.S., 2024. Spatial downscaling of the GCMs precipitation product over various regions of Iran: application of long short-term memory model. Phys. Chem. Earth, Parts A/B/C 136, 103768. https://doi.org/10.1016/j.pce.2024.103768.

Kheyruri, Y., Neshat, A., Sharafati, A., Hameed, A.S., 2024. Identifying the most effective climate parameters on crop yield in rain-fed agriculture and irrigated farming in Iran. Phys. Chem. Earth, Parts A/B/C 136, 103744. https://doi.org/10.1016/j.pce.2024.103744.

Lawa, F.A., 2004. Sequence Stratigraphic Analysis of the Middle Paleocene-Middle Eocene in the Sulaimani District (Kurdistan Region). College of Science, University of Sulaymaniyah, Iraq. Unpublished Ph. D. Thesis.

Le Pichon, X., Sibuet, J.C., 1981. Passive margins: a model of Formation. J. Geophys. Res. 86 (B5), 3708–3720. https://doi.org/10.1029/JB086iB05p03708.

McKenzie, D.P., 1974. Some remarks on the development of sedimentary basins. Earth Planet Sci. Lett. 40, 25–32.

Naderi, G., Karimzadeh, S., 2024. Seismic hazard assessment of the Sulaymaniyah Region, Northeastern Iraq: a probabilistic and deterministic approach. Nat. Hazards 120, 1–25.

Nissen, E., et al., 2023. The 2017 Mw 7.3 Sarpol-e Zahab (Iran-Iraq) earthquake: new constraints on fault geometry and slip distribution from InSAR and teleseismic data. Geophys. Res. Lett. 50 e2022GL101987.

Numan, N.M.S., 1997. A plate tectonic scenario for the Phanerozoic succession in Iraq. Iraqi Geological Journal 30, 85–119.

Numan, N.M.S., Al-Azzawi, N.K.B., 1993. Structural and geotectonic interpretation of vergence directions of anticlines in the foreland folds of Iraq. In: Abhath Al-Yarmouk, (Pure Science and Engineering), 2. Yarmouk University, Jordan, pp. 57–73.

Numan, N.M.S., Al-Azzawi, N.K.B., 2002. Progressive versus paroxysmal alpine folding in sinjar anticline, northern Iraq. Iraqi Jour. of Earth Science.

Onur, T., Gok, R., Abdlnaby, W.G., Mahdi, H., Numan, N.M.S., Al-Shukri, H., Shakir, A. M., Ghlaib, H.K., Ameen, T.H., Abd, N.A., 2017. Comprehensive earthquake catalog for Iraq in terms of moment magnitude. Seismol Res. Lett. 88 (No.3).

Rakib, M.M.H., Khan, R., Khan, A., Ovi, M.H., Biswas, P.K., Islam, M.S., Akbar, M.A., Mallick, J., Hang, H.T., Roy, D.K., 2026. Geochemical insights into the depositional environment dynamics of Gondwana sediments in the Tajpur basin, Bangladesh. Phys. Chem. Earth, Parts A/B/C 142, 104300. https://doi.org/10.1016/j.pce.2026.104300.

Sharland, P.R., Archer, R., Casey, D.M., Hall, S.H., Heward, A.P., Horbury, A.D., Simmons, M.D., 2001. In: AP Sequence Stratigraphy, 2. GeoArabia, Special Publication, Gulf Petrolink, Bahrain, p. 371.

Sissakian, V.K., Fouad, S.F., Al-Ansari, N., Knutsson, S., 2014. Deformational style of the soft sediment (SEISMITES) within the uppermost part of the euphrates formation, Western Iraq, jour. of Earth Sciences and Geotechnical Engineering 4 (4), 71–86. ISSN: 1792-9040 (print), 1792-9660 (online).